

Figure S1, related to Figure 1. Increased glucose metabolism fuels gemcitabine resistance in Gem-R pancreatic cells. (A) Relative clonogenicity of Gem-R as compared to WT cells on day 21 after plating. (B) Average colony size and colony number in Gem-R vs. WT cells as determined by soft agar assays. Colony number and size was determined by pictomicrography, and plotted for WT and Gem-R. (C) Relative survival in response to gemcitabine treatment in MIA PaCa-2 Gem-R cells as compared to the WT cells as determined by MTT cytotoxicity assays. Cells were treated for 72 hr. (D-E) Relative glucose uptake (D) and lactate release (E) in MIA PaCa-2 Gem-R vs. WT cells, cultured under normoxia (20% O₂) or hypoxia (1% O₂). Raw values were normalized to cell counts and plotted as a percent of normoxic WT controls. (F-I) Relative cell survival under low glucose or 2-DG in AsPC-1 (F-G) and MIA PaCa-2 (H-I) cell lines as determined by MTT assays. Cell survival was measured after 48 hr of treatments. (J) ECAR, OCR, and OCR/ECAR ratios in WT, Gem-R, and partially resistant (PR) Gem-R cells. (K-L) ECAR (K) and OCR (L) levels in WT and partially resistant (cells with gemcitabine IC50 values in between WT and Gem-R cells; PR) Gem-R cells under treatment with 2,4-DNP, 2-DG, and rotenone. (M) Relative *GLUT1* expression in WT, Gem-R, and Gem-R cells sorted for low surface GLUT1 expression, plotted relative to WT controls, as determined by qPCR. (N) Relative responsiveness of WT and Gem-R cells to metformin and oligomycin at 72 hr post-treatment by MTT assays. For all in vitro studies n=3 per sample. Data are represented as mean ± SEM. The bar charts in panel B and J were compared by Student's t-test. The data in panel D, E, F, G, H, I, and M were compared by one-way ANOVA. Data in panel N was compared by one-way ANOVA followed by Tukey's post hoc test. * p < 0.05, ** p < 0.01, and *** p < 0.001.

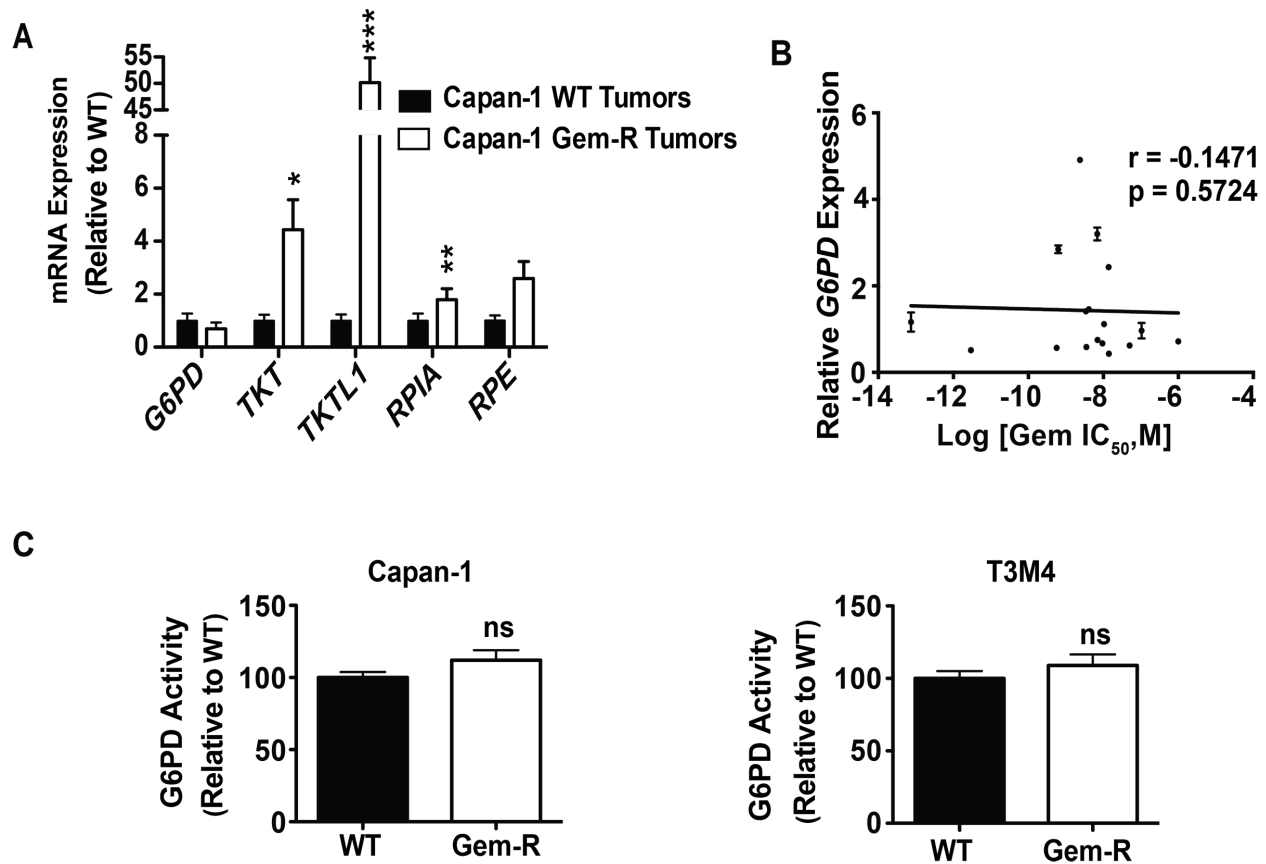


Figure S2, related to Figure 2. Decreased carbon flux through oxidative PPP in Gem-R cells. (A) qPCR analysis of PPP enzymes in Capan-1 WT and Gem-R tumors. (B) Pearson's correlation coefficient analysis of G-6-PD expression with gemcitabine IC₅₀ in 17 pancreatic cancer cell lines after 72 hr treatment. (C) G-6-PD activity assay in Gem-R cells as compared to WT cells. For all in vitro studies n=3 per sample. Data are represented mean \pm SEM. The bar graphs in panel A and C were compared by using Student's t-test. * p < 0.05, ** p < 0.01, and *** p < 0.001.

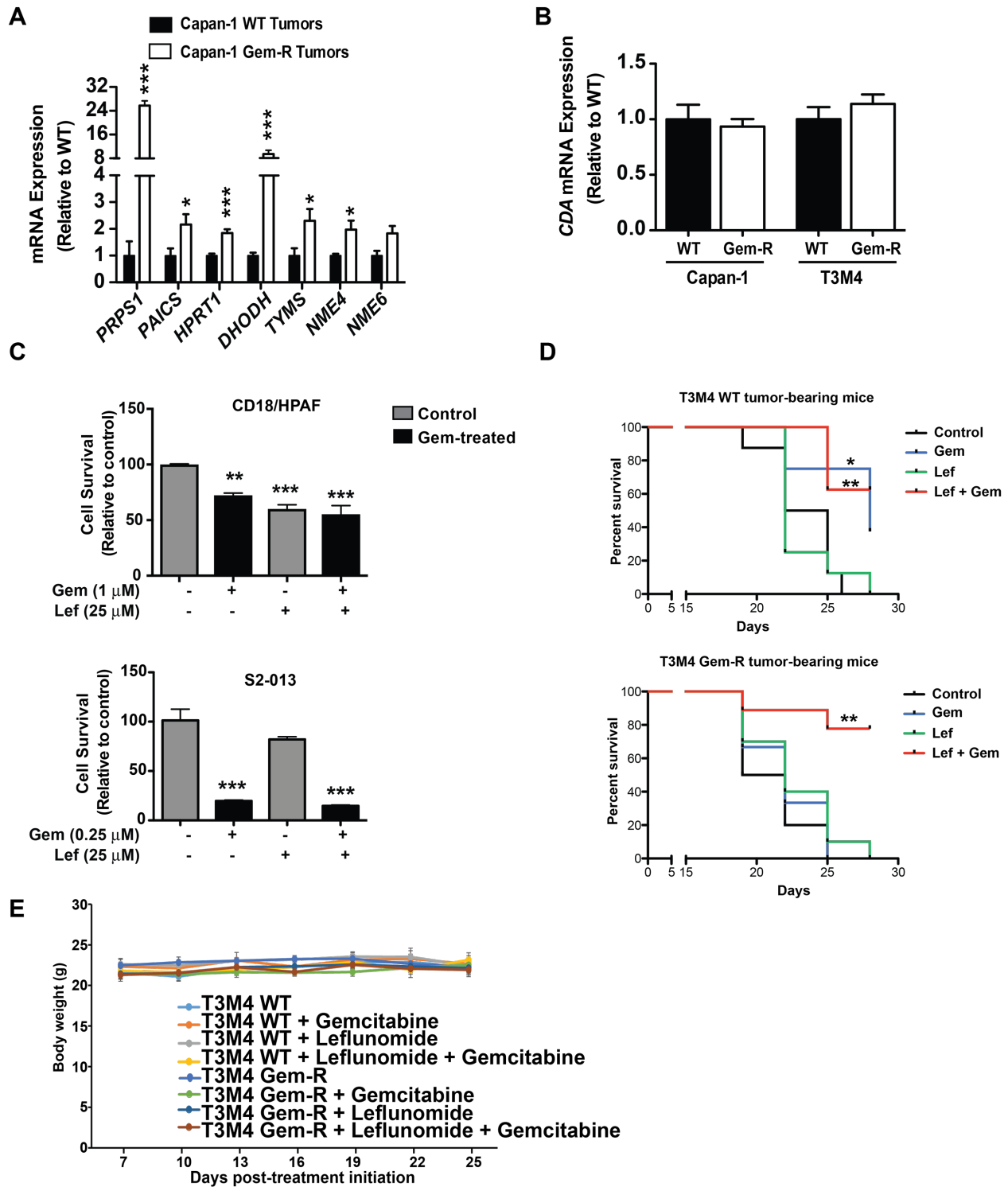


Figure S3, related to Figure 3. De novo pyrimidine synthesis is significantly upregulated in Gem-R cells. (A) Relative mRNA levels of enzymes involved in pyrimidine biosynthesis pathway in tumors from WT and Gem-R cell-implanted mice, as

determined by qPCR and plotted relative to WT controls. Tumor samples were collected after 28 days of implantation of cells. (B) Relative mRNA levels of *CDA* in WT and Gem-R cells, as determined by qPCR and plotted relative to WT controls. (C) Relative survival of S2-013 and CD18/HPAF cells under treatment with control, leflunomide (Lef) and/or gemcitabine (Gem) for 72 hr. (D) Kaplan-Meier survival analysis of mice orthotopically implanted with T3M4 WT and Gem-R cells and treated with control, gemcitabine (Gem), leflunomide (Lef), or the combination of gemcitabine and leflunomide (Lef + Gem). In WT control 8, gemcitabine 8, leflunomide 8 and combination of leflunomide with gemcitabine 8 mice were used. In Gem-R control 10, gemcitabine 9, leflunomide 10 and combination of leflunomide with gemcitabine 10 mice were used. Statistical comparisons were done with Log-rank (Mantel-Cox) test. (E) Body weight of mice with the indicated treatments. For all in vitro studies n=3 per sample. Data are represented mean \pm SEM. The bar graphs in panel A and B were compared by using Student's t-test. Bar graphs in panel C were compared by using one-way ANOVA. * p < 0.05, ** p < 0.01, and *** p < 0.001.

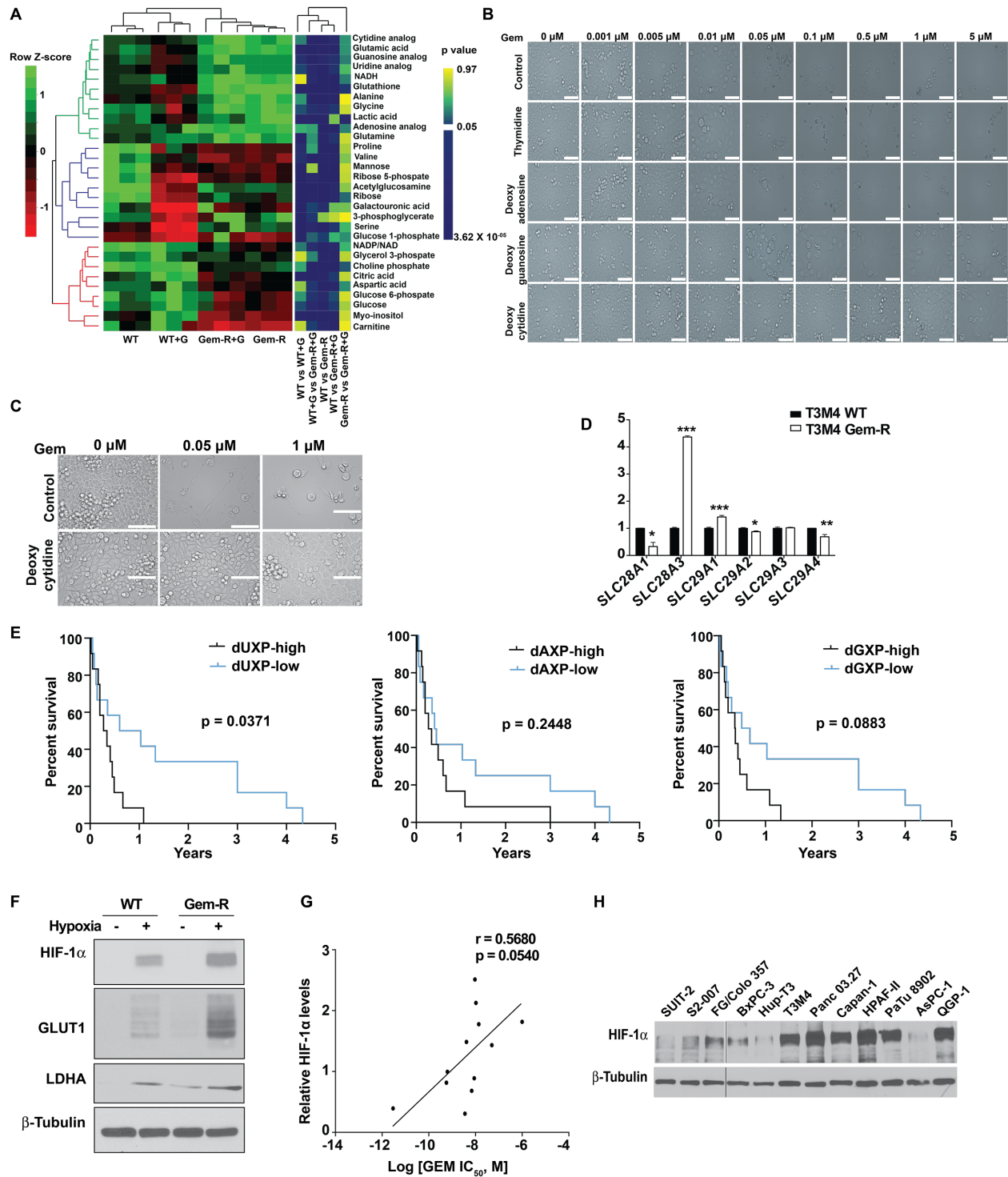


Figure S4, related to Figure 4 and Figure 5. Deoxycytidine and HIF-1α increase gemcitabine resistance in multiple pancreatic cancer cell lines. (A) Heat map demonstrating unsupervised hierarchical clustering and major metabolic alterations in

Capan-1 WT and Gem-R cells, under control or gemcitabine treated conditions, identified by ^1H - ^{13}C HSQC NMR analysis. Left panel denotes the relative concentration change of metabolites in the cell lysates collected from triplicate samples of WT, gemcitabine-treated WT (WT+G), Gem-R and gemcitabine-treated Gem-R (Gem-R+G) cells. The color code extends from red to green as the relative level of a metabolite increases. The top hierarchical clustering pattern was calculated using the overall metabolite alteration in each sample. Metabolites clustered in the green colored group (green horizontal lines on the left side of the heat map) increased in GEM-R cells irrespective of gemcitabine treatment, while metabolites clustered in the red colored group decreased in Gem-R cells. The blue clustered metabolites are altered in WT cells upon gemcitabine treatment. The right panel heat map denotes p-values for metabolic alterations in the indicated groups. (B) Effect of deoxycytidine treatment on gemcitabine sensitivity in S2-013 cells and (C) MIA PaCa-2 cells as demonstrated by pictomicrography. Cell were treated for 72 hr. (D) qPCR expression of various transporters involved in nucleoside and gemcitabine transport plotted as fold change of WT control \pm SEM. G: gemcitabine; *SLC29A1-4*: equilibrative nucleoside transporters; *SLC28A1-3*: concentrative nucleoside transporters. (E) Kaplan-Meier progression-free survival analysis of PDAC patients on gemcitabine/5-FU chemotherapy with high (above median, n=12) or low (below median, n=12) dUXP, dAXP, or dGXP levels, as determined by LC-MS/MS in human pancreatic tumors. (F) Immunoblotting to determine the levels of HIF-1 α and HIF-1 α -dependent metabolic gene products in MIA PaCa-2 WT vs. Gem-R cells. (G) Pearson's correlation between HIF-1 α protein levels with the IC_{50} of gemcitabine. All the cell lines are indicated in panel H. (H) Protein levels of HIF-1 α in 12 pancreatic cancer cell lines. For all in vitro studies n=3 per sample. Data are represented mean \pm SEM. The bar graphs in panel D were compared by using Student's t-test. Scale bars indicate 100 μm . * p < 0.01 ** p < 0.01, and *** p < 0.001 as compared to WT controls.

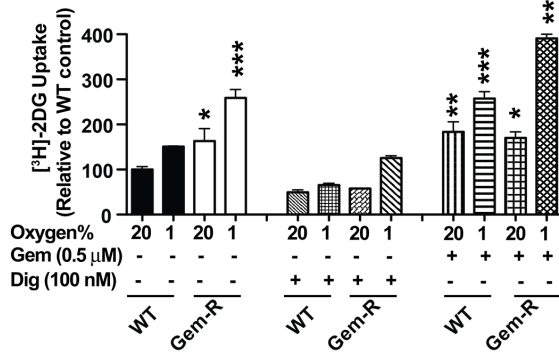
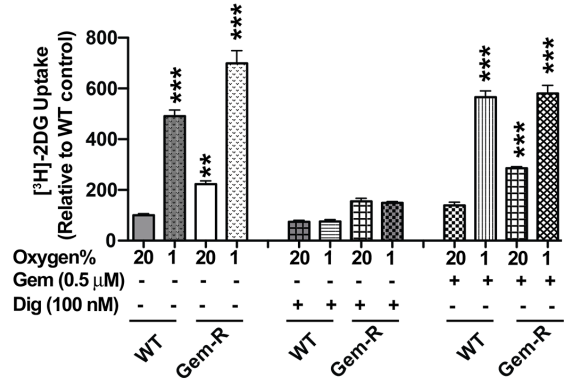
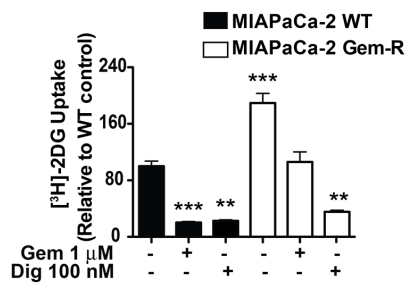
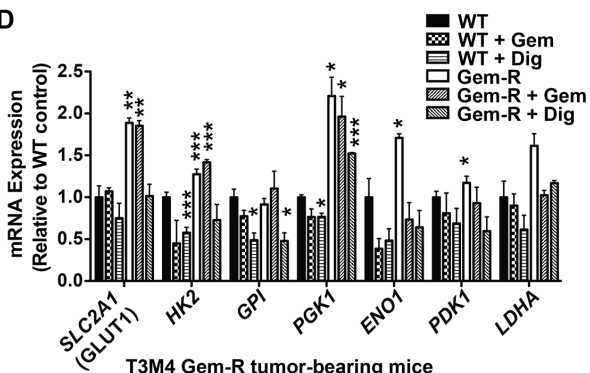
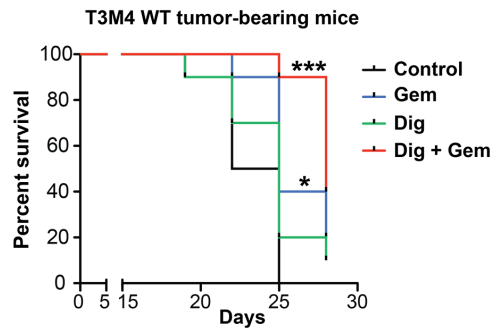
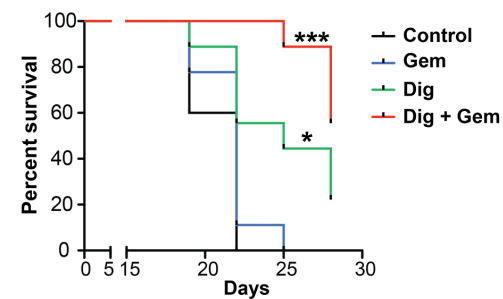
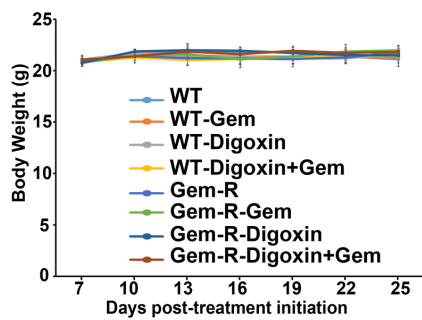
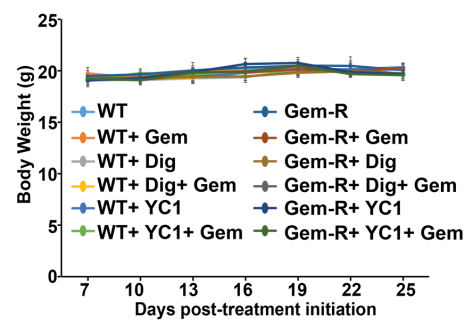
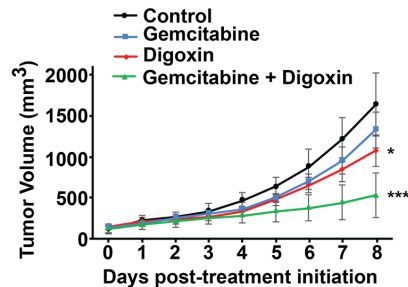
A**B****C****D****E****F****F****G****H**

Figure S5, related to Figure 6. Pharmacological inhibition of HIF-1 α diminishes glucose uptake and glycolytic gene expression. (A-B) Relative glucose uptake in T3M4 (A) and Capan-1 (B) Gem-R vs. WT cells under indicated treatments. Dig: digoxin; Gem: gemcitabine. Raw values were normalized to cell counts and plotted as percent of normoxic WT controls. (C) Relative effect of digoxin treatment on glucose uptake as determined by [3 H]-2DG uptake in WT and Gem-R MIAPaCa-2 cells. Scintillation counts were normalized to cell counts and plotted as percent of untreated WT control. (D) Relative expression of glycolytic genes under gemcitabine or digoxin treatment in Capan-1 WT and Gem-R cells, as determined by qPCR and plotted relative to untreated WT controls. Dig: digoxin; Gem: gemcitabine. The values are presented \pm S.E.M. (E) Kaplan-Meier survival analysis of mice orthotopically implanted with T3M4 WT and Gem-R cells and treated with control, gemcitabine (Gem), digoxin (Dig), or the combination of gemcitabine and digoxin (Dig + Gem). In WT control 10, gemcitabine 9, digoxin 10 and combination of digoxin with gemcitabine 10 mice were used. In Gem-R control 10, gemcitabine 9, digoxin 9 and combination of digoxin with gemcitabine 9 mice were used. Statistical comparisons were done with Log-rank (Mantel-Cox) test. (F-G) Body weight of mice implanted with WT and Gem-R T3M4 (F) and Capan-1 (G) cells with the indicated treatments. (H) Effect of digoxin on gemcitabine responsiveness in PATX162 patient-derived xenograft. For all in vitro studies n=3 per sample. Data are represented mean \pm S.E.M. Bar graph in panel A, B, C and D were compared by using one-way ANOVA. * p < 0.05, ** p < 0.01, and *** p < 0.001.

Table S1, related to Figure 1, 4, and 8

Patient Characteristics	Category	Frequency (number)
Cohort 1		
Age (years)	40-49	20% (5)
	50-59	20% (5)
	60-69	16% (4)
	70-79	32% (8)
	80+	12% (3)
Stage	2-2.5	8% (2)
	3-3.5	48% (12)
	4	36% (9)
	unknown	8% (2)
Sex	Male	56% (14)
	Female	44% (11)
Cohort 2		
Age (years)	40-49	4.2% (1)
	50-59	20.8% (5)
	60-69	25.0% (6)
	70-79	41.7% (10)
	80+	8.3% (2)
Grade	1-1.5	4.2% (1)
	2-2.5	25.0% (6)
	3-3.5	45.8% (11)
	4	25.0% (6)
Sex	Male	79.2% (19)
	Female	20.8% (5)
Cohort 3		
Age (years)	40-49	3.2% (1)
	50-59	22.6% (7)
	60-69	32.3% (10)
	70-79	29% (9)
	80+	12.9% (4)
Grade	2-2.5	32.3% (10)
	3-3.5	32.3% (10)
	4	35.4% (11)
Sex	Male	77.4% (24)
	Female	22.6% (7)

Table S2, related to Figure 3

List of PPP and nucleotide biosynthesis genes compared between Capan-1 WT (WT) and Capan-1-Gem-R (Gem-R) cells.

Replicate 1			Replicate 2				
Genes	Expression in Gem-R	Expression in WT	Ratio of Medians (Gem-R/WT)	Genes	Expression in Gem-R	Expression in WT	Ratio of Medians (Gem-R/WT)
<i>G6PD</i>	4333	3626	1.2	<i>G6PD</i>	4005	3362	1.2
<i>H6PD</i>	209	211	1.0	<i>H6PD</i>	247	236	1.0
<i>PGLS</i>	998	950	1.1	<i>PGLS</i>	1069	1065	1.0
<i>PRPS1</i>	426	567	0.7	<i>PRPS1</i>	564	640	0.8
<i>PRPS1L1</i>	113	121	0.8	<i>PRPS1L1</i>	112	123	0.7
<i>PRPS2</i>	659	736	0.9	<i>PRPS2</i>	777	722	1.1
<i>RBKS</i>	177	172	1.0	<i>RBKS</i>	231	192	1.2
<i>RPE</i>	2976	2141	1.4	<i>RPE</i>	2851	2107	1.4
<i>RPIA</i>	3173	2288	1.4	<i>RPIA</i>	2120	1780	1.2
<i>TKTL1</i>	78	86	0.6	<i>TKTL1</i>	111	83	3.3
<i>TKTL2</i>	124	90	0.9	<i>TKTL2</i>	87	74	1.0
<i>TKT</i>	53192	21266	2.5	<i>TKT</i>	42392	20545	2.1
<i>ATIC</i>	4191	3494	1.2	<i>ATIC</i>	4497	3751	1.2
<i>IMPDH1</i>	1518	1162	1.3	<i>IMPDH1</i>	1344	1202	1.1
<i>APRT</i>	5764	4191	1.4	<i>APRT</i>	4950	4156	1.2
<i>HPRT1</i>	5948	6082	1.0	<i>HPRT1</i>	6621	6684	1.0
<i>ADA</i>	494	316	1.7	<i>ADA</i>	590	354	1.8
<i>DHODH</i>	1105	838	1.3	<i>DHODH</i>	1288	890	1.5
<i>UMPS</i>	615	542	1.1	<i>UMPS</i>	686	678	1.0
<i>CTPS</i>	1815	1248	1.5	<i>CTPS</i>	2147	1354	1.6
<i>CTPS2</i>	483	435	1.1	<i>CTPS2</i>	560	507	1.1
<i>TYMS</i>	1941	1265	1.6	<i>TYMS</i>	1900	1230	1.6
<i>DHFRL1</i>	89	83	1.0	<i>DHFRL1</i>	101	80	1.3
<i>CMPK1</i>	1178	1381	0.8	<i>CMPK1</i>	1559	1577	1.0
<i>NME1</i>	11749	7273	1.6	<i>NME1</i>	10012	6930	1.4
<i>NME2</i>	79	81	0.7	<i>NME2</i>	110	79	1.1
<i>NME3</i>	1099	936	1.2	<i>NME3</i>	1212	1012	1.2
<i>NME4</i>	37853	15831	2.4	<i>NME4</i>	23298	13869	1.7
<i>NME5</i>	78	91	0.4	<i>NME5</i>	104	100	0.8
<i>NME6</i>	428	352	1.2	<i>NME6</i>	376	348	1.1
<i>NME7</i>	1356	1066	1.3	<i>NME7</i>	1487	1120	1.3
<i>TK2</i>	617	480	1.3	<i>TK2</i>	582	509	1.1
<i>PRPS1</i>	426	567	0.7	<i>PRPS1</i>	564	640	0.8
<i>PRPS1L1</i>	113	121	0.8	<i>PRPS1L1</i>	112	123	0.7
<i>PRPSAP1</i>	1683	1084	1.6	<i>PRPSAP1</i>	1977	1222	1.6
<i>PRPSAP2</i>	261	257	1.0	<i>PRPSAP2</i>	307	303	0.9
<i>PPAT</i>	623	600	1.0	<i>PPAT</i>	599	634	0.9
<i>GART</i>	236	204	1.2	<i>GART</i>	246	204	1.1
<i>PFAS</i>	5381	4077	1.3	<i>PFAS</i>	4475	3801	1.2
<i>PAICS</i>	16176	14469	1.1	<i>PAICS</i>	16747	14739	1.1
<i>ADSL</i>	2474	2055	1.2	<i>ADSL</i>	2294	1944	1.2

Genes demonstrating expression above 500 (arbitrary units) with both Gem-R and WT cells, and a ratio of 1.5 or above in both replicates were selected for further analysis and are indicated in red.